AD-A183 401 LOW TEMPERATURE STUDIES OF ANOMALOUS SURFACE SHIELDING AND RELATED PHENOMENA(U) STANFORD UNIV CA DEPT OF PHYSICS W M FAIRBANK 14 NOV 86 AFOSR-TR-87-0923 1/1

UNCLASSIFIED AFOSR-85-0023 F/G 9/7 NL

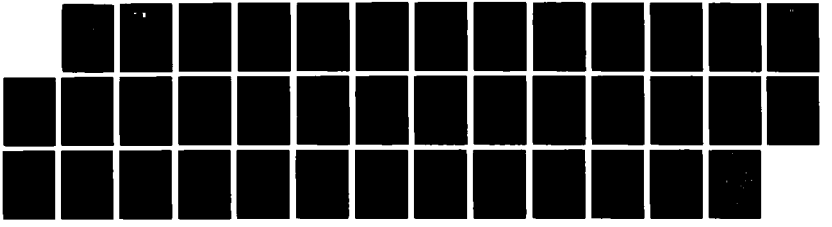

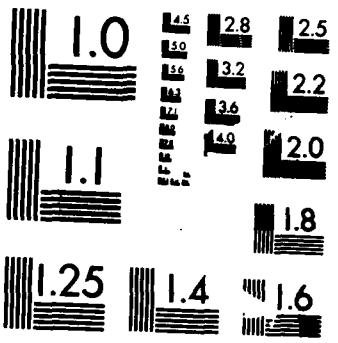

UNCLASSIFIED UTIC FILE COPY

SECURITY CLASSIFICATION OF THIS PAGE

DTIC FILE COPY (2)

REPORT DOCUMENTATION PAGE

DTIC ELECTE D OCT 05 1987

AD-A183 401

1a. REPORT SECURITY CLASSIFICATION: Unclassified	1b. RESTRICTIVE MARKINGS
2a. SECURITY CLASSIFICATION AU[illegible]	3. DISTRIBUTION/AVAILABILITY OF REPORT: Approved for public release, distribution unlimited
[illegible]UMBER(S)	5. MONITORING ORGANIZATION REPORT NUMBER(S): AFOSR-TR- 87-0923
6a. NAME OF PERFORMING ORGANIZATION: Standford University	6b. OFFICE SYMBOL (If applicable):
6c. ADDRESS (City, State and ZIP Code): Department of Physics, Standford University, Standford, CA 94305	7b. ADDRESS (City, State and ZIP Code): Building 410, Bolling AFB, Wash D.C. 20332-6448
8a. NAME OF FUNDING/SPONSORING ORGANIZATION: AFOSR	8b. OFFICE SYMBOL (If applicable): NP
8c. ADDRESS (City, State and ZIP Code): Bldg 410, Bolling AFB, Wash D.C. 20332-6448	9. PROCUREMENT INSTRUMENT IDENTIFICATION NUMBER: AFOSR-85-0023
	10. SOURCE OF FUNDING NOS.

PROGRAM ELEMENT NO.	PROJECT NO.	TASK NO.	WORK UNIT NO.
61102F	2301	A8	

11. TITLE (Include Security Classification): "LOW TEMPERATURE STUDIES OF ANOMALOUS SURFACE SHIELDING AND RELATED PHENOMENA"

12. PERSONAL AUTHOR(S): Dr. William M. Fairbank

13a. TYPE OF REPORT	13b. TIME COVERED	14. DATE OF REPORT (Yr., Mo., Day)	15. PAGE COUNT
FINAL	FROM 84/11/15 TO 86/11/14		37

16. SUPPLEMENTARY NOTATION

17. COSATI CODES			18. SUBJECT TERMS (Continue on reverse if necessary and identify by block number)
FIELD	GROUP	SUB. GR.	Low Temperature, Surface Shielding, Positron Weight

19. ABSTRACT (Continue on reverse if necessary and identify by block number)

Experiments were conducted to determine the force of gravity on positrons and electrons. An anomalous, low temperature shielding effect was discovered in copper and studied. (Two graduate students received their PhD, during this period. It is believed that sharp increases in the microwave surface conductivity of copper and aluminum are caused by the appearance of a high mobility surface layer at low temperatures

20. DISTRIBUTION/AVAILABILITY OF ABSTRACT	21. ABSTRACT SECURITY CLASSIFICATION
UNCLASSIFIED/UNLIMITED ☐ SAME AS RPT. ☒ DTIC USERS ☒	UNCLASSIFIED

22a. NAME OF RESPONSIBLE INDIVIDUAL	22b. TELEPHONE NUMBER (Include Area Code)	22c. OFFICE SYMBOL
ROBERT J. BARKER	202/767-5011	NP

DD FORM 1473, 83 APR EDITION OF 1 JAN 73 IS OBSOLETE. UNCLASSIFIED

SECURITY CLASSIFICATION OF THIS PAGE

Department of Physics
Stanford University
Stanford, CA 94305

FINAL REPORT

to the

AIR FORCE OFFICE OF SCIENTIFIC RESEARCH

for

LOW TEMPERATURE STUDIES OF ANOMALOUS SURFACE SHIELDING AND RELATED PHENOMENA

Air Force Contract # AFOSR 85-0023

For the Period: 11-15-84 to 11-14-86

Principal Investigator:
William M. Fairbank
Professor of Physics

We have been working on an experiment to determine the force of gravity on positrons and electrons. We have also been investigating the anomalous shielding effect in copper discovered during the course of that work. Three graduate students have been working on this project: John Henderson and Wayne Rigby, whose theses are enclosed as Appendices A and B to this report, and Mark Rzchowski, who is currently working on his thesis. We proposed a cooperative experiment working with Lawrence Livermore National Laboratory and we have included it as Appendix C. Appendix D, submitted to the 18th International Conference on Low Temperature Physics, August 1987, is a paper summarizing our work on the copper shielding effect.

APPENDIX C

Contents

Abstract

We propose to modify the apparatus used to measure the gravitational acceleration of electrons[1] to make the same measurements on positrons in a cooperative effort with the Lawrence Livermore National Laboratory, and to make electron measurements with the modified apparatus at Stanford. This will be the first comparison of the gravitational acceleration of matter and antimatter, and will test several current theories of this fundamental interaction[2]. We also intend to investigate further the extraordinarily small ambient electric fields observed in the experiment at low temperatures. These investigations involve measurements of the microwave surface impedance and DC surface potential of metals at low temperatures.

In section 1 we present a brief discussion of the results obtained on electrons with the gravitational force apparatus. Section 2 describes the apparatus and the modifications necessary to make it compatible with the positron source at Livermore. We also discuss a technique to decrease the energy spread of the incoming beam. Sections 3 and 4 describe the two measurement techniques employed in the gravitational force experiment: the time of flight technique and the movable drift tube technique. The first method takes advantage of the small ambient fields observed at low temperature, while the second is independent of this effect. We show that both of these methods are capable of 1% accuracy with three hours of data taking. Section 5 presents our surface impedance and surface potential investigations into a shielding effect that may be responsible for the observed small ambient fields. We observe low temperature anomalies in the microwave surface impedance of copper and aluminum, and propose a surface potential measurement in an operational apparatus to correlate the anomalies with a shielding effect.

SECTION 1 - HISTORICAL BACKGROUND

Motivated by the desire to measure for the first time the force of gravity on antimatter, Witteborn and Fairbank (WF)[1] developed a low temperature apparatus to measure the force of gravity on individual electrons and positrons. That experiment [3] successfully measured the force of gravity on electrons.

The force of gravity on an electron is extremely small. In order to make the measurement it is necessary to provide electrostatic shielding from external electric fields. This is accomplished by using a copper drift tube for the electrons to travel through. There are two background effects that were expected to contribute forces much larger than the measured force. The patch effect, which is due to the polycrystalline nature of the drift tube, was expected to be around 10^4 *mg* to 10^5 *mg*. An overall potential gradient between 10^{-6} V/m and 10^{-5} V/m (10^4 *mg* to 10^5 *mg*) due to gravitational sagging of the drift tube was also expected. (Both effects will be discussed in the next section.)

Measurements were made with two methods. The movable drift tube method gives the gravitational force on the electron <u>independent</u> of the background forces on the electron while it is in the drift tubes. (This will be discussed in detail later.) To make the time-of-flight (TOF) measurements, a pulse of low energy electrons was repeatedly shot upward through a 0.9m long drift tube. Their transit times were determined by measuring their time of arrival at a photomultiplier tube relative to the time the pulse of electrons was launched. The photomultiplier tube is above the drift tube. Knowing the initial energy distribution of the pulse and the number seen at the detector as a function of time, the net force on the electron while it is in the drift tube can be determined. (This method is discussed further in section III.) The TOF method can only measure the net force on the test particle. This means that the TOF method cannot measure the gravitational acceleration of the electron and the positron independently. If F_1 is the net force measured on the electron, and $\mathbf{E}$ is the ambient electric field in the drift tube, then (taking up to be positive)

(1) $\quad -mg - e\mathbf{E} = F_1 \quad .$

where m is the inertial mass of the electron, e is its charge, and g is its gravitational acceleration. Similarly, with g' the gravitational acceleration of the positron and F_2 the measured net force,

(2) $\quad -mg' + e\mathbf{E} = F_2 \quad .$

Adding equations (1) and (2), we obtain

(3) $\quad -m\,(g+g') = F_1 + F_2 \quad .$

Since there are three unknowns (g, g', and $\mathbf{E}$) and only two fundamental equations [(1) and (2)], it is not possible to solve for both gravitational forces directly. However, using the accepted value of g for the electron, the force of gravity on the positron can be found from equation (3). The accuracy of that value depends on the accuracy to which F_1 and F_2 are known. Since the term $\pm e\mathbf{E}$ cancels from F_1 and F_2, it is advantageous to have $e\mathbf{E}$ (hence F_1 and F_2) as small as possible. (One needs the uncertainty in F_1 and F_2 to be smaller than mg. The larger $e\mathbf{E}$ is, the smaller the relative uncertainty in F_1 and F_2 has to be.)

Using the movable drift tube technique, WF measured the accepted value of g for the electron to 30%. With the TOF technique, they found the net force on the electron in the drift tube to be $0.00\pm0.09\ mg$. This low value of the net force makes it easier to measure the force of gravity on positrons. These experiments were performed at 4.2K to use low-noise superconducting electronics.

To discover why these background forces were not present at 4.2K, the apparatus was modified to operate at a variety of temperatures. Lockhart, Witteborn, and Fairbank[4] found a sharp change in the net force at 4.5K, from essentially zero to a value consistent with the theoretically expected forces of approximately $10^4\ mg$. To account for this behavior, a shielding effect that would screen out the large forces was proposed. Recent results with microwave cavities (discussed later) indicate that the effect may take place on aluminum surfaces as well as on copper surfaces. An experiment to look at the shielding effect directly has been constructed and tested (see section V).

The original motivation of comparing the force of gravity on matter and antimatter is even stronger than before. In addition to the fundamental nature of the measurement, there is now the possibility that the force of gravity may be <u>different</u> on anitmatter[2].

During the last few years there has been a rapid growth of experiments which use low energy positrons to study a wide variety of problems. Some of this work has become possible due to the development of a linear accelerator as a high intensity positron source[5]. Such a source makes it feasible to measure the force of gravity on positrons. In addition to giving the first measurement of the force of gravity on antimatter, such an experiment would also give a definitive value for the electrostatic sheilding seen in the drift tube below 4.5K.

SECTION 2 - MODIFICATIONS TO THE GRAVITATIONAL FORCE EXPERIMENT

The major effort required will be to modify the present working apparatus to accomodate the positron beam. A technique to reduce the energy spread of the incoming beam will be implemented to enhance the data rate.

The methods used to reduce background forces have been extensively discussed in the litterature[1,3] and will only be discussed briefly here. All of the conditions described in this paragraph have been met successfully in the original electron experiment. A metal tube needs to be used as the test region to prevent static charge buildup and shield external fields from the drift region. Particles (electrons or positrons) displaced from the tube axis feel an attractive force to the nearest tube wall due to an asymmetrical image charge distribution. This is minimized by using an axial magnetic field to prevent the particles from drifting off axis. Thermally induced electric fields are reduced below 0.1 *mg/e* by using a thick walled drift tube and having only one point of thermal contact with the liquid helium bath. Thermal fluctuations in the electric field due to 4.2K black body radiation are on the order of 10^{-4} *mg/e*.[7] Variations in the magnetic field used to guide the particles can cause variations in the kinetic energy of the particle. Using the present magnet system and selecting particles with the lowest cyclotron energy (lowest magnetic state), these fluctuations can be reduced to 10^{-3} *mg/e*. Interactions with residual gas can be reduced to an acceptable level by keeping the pressure below 3×10^{-11} torr at 4.2K.

The fact that the drift tubes themselves are in a gravitational field results in an induced electric field along the tube axis. This is due to sagging of both the electrons and the ion cores in the metal. The original theoretical prediction by Schiff and Barnhill[8] was that a downward electric field of amplitude *mg/e* would be produced. Since this just cancels the gravitational force for an electron, the net force on an electron would be zero, consistent with the WF results at 4.2K. A different

derivation by Dessler *et. al.*[9] predicted the field should be around 0.2 *Mg/e* upward (*M* is the ion mass). The discrepancy between the two predictions was resolved by Herring[10] when he showed that the result of Dessler *et. al.* could be obtained using the approach of Schiff and Barnhill by taking into account certain surface effects. The expected field is then approximately 10^4 *mg/e*, which is consistent with the experimental results above 4.5K, but not below 4.5K.

The drift tube is made of many crystallites. The inside surface of the drift tube will have random crystal faces exposed, so the potential on the surface will vary also. This leads to a variation in the potential on the axis of the tube. The rms potential variation on the axis, $\langle\Phi^2\rangle^{1/2}$, is[11]

$$\langle\Phi^2\rangle^{1/2} = 0.26\ (w/r)\ \phi \quad ,$$

where w is the mean crystallite width on the surface, r is the tube radius, and ϕ is the rms variation of the surface potential. In this experiment, $w \approx 10^{-4}$ cm, r = 2.5 cm, and $\phi \approx 0.1$ V. Then $\langle\Phi^2\rangle^{1/2} \approx 10^{-6}$ V (or forces of approximately 10^5 *mg*). Again, this is consistent with the results above 4.5K, but not below 4.5K.

These last two effects are only relevant to the TOF technique. Figure 2.1 shows a diagram of the modified apparatus. The modified apparatus differs from the original apparatus in that the detector is at the bottom instead of the top, the source of particles is now brought in through the top and can therefore be changed, a velocity selector tube has been added to narrow the energy distribution of the incoming particles, and the system of guide magnets must be altered to account for the above changes.

Operation of the system begins with a 10 nanosecond bunch of more than 10^6 positrons from the Lawrence Livermore National Laboratory (LLNL) linac.[12] The bunch has an average energy of ~10^3 eV and an energy spread of a few eV. To lower the energy spread, the beam will be brought in at an angle to the main guiding magnetic field so as to impinge upon the rethermalizer. The rethermalizer is a cooled crystal of copper. The positrons embed in the rethermalizer and diffuse back out due to the negative work function of positrons in the rethermalizer. Some of the positrons

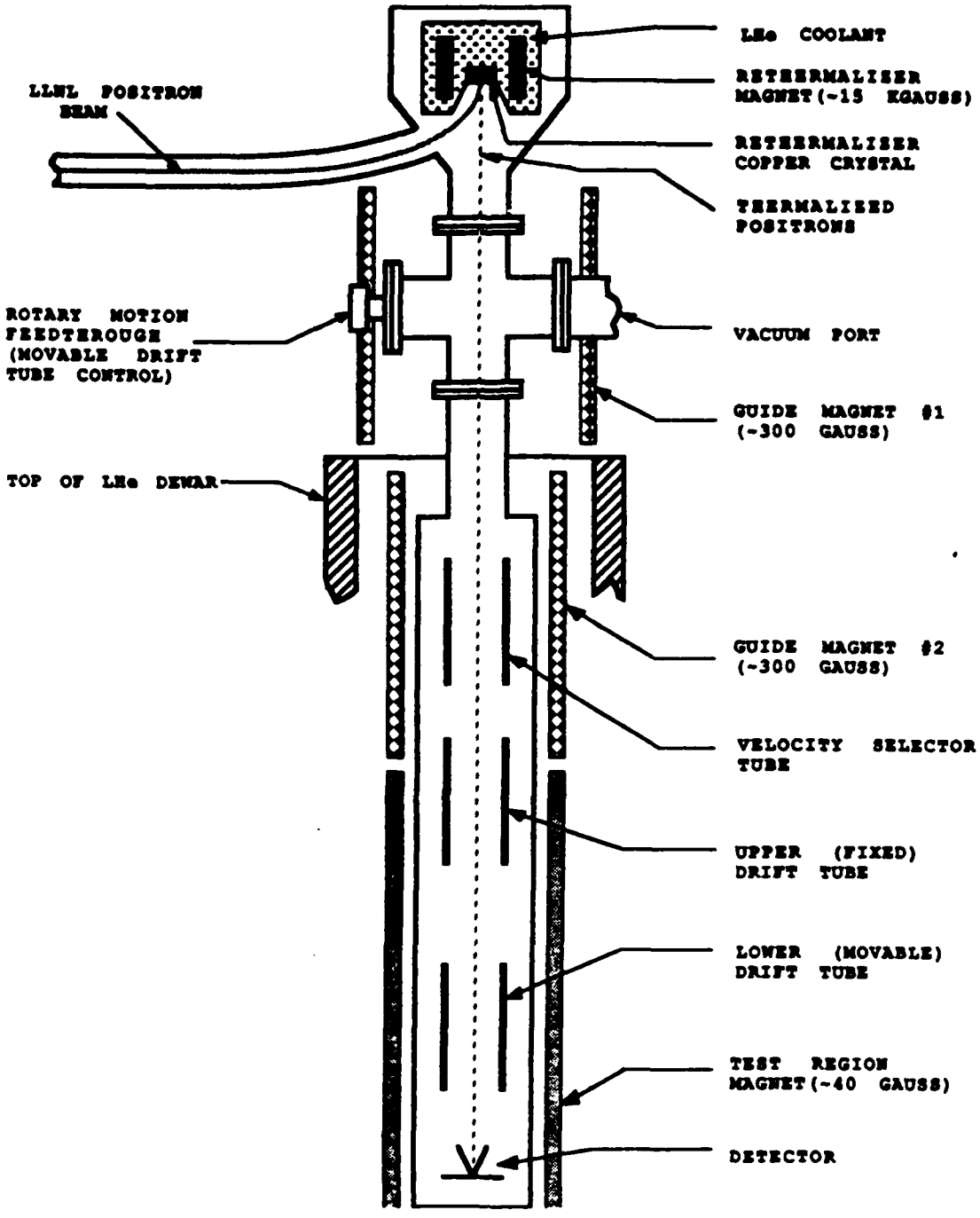

Fig. 2.1 Scematic diagram of the modified apparatus. The work covered in this proposal is for the developement and testing of the apparatus below the positron rethermalizer.

annihilate with electrons in the crystal. The remaining 10% to 40% of the positrons rethermalize by collisions in the crystal. Rethermalization has been demonstrated[13] at temperatures below 20K. By cooling the rethermalizer to 4.2K (or below) we should be able to reduce the spread of energy (perpendicular to the crystal face) of the reemitted positrons to ~0.5×10^{-3} eV. In order to preferrentially populate the lowest magnetic states (lowest cylotron energy), the magnetic field needs to be high in the region of rethermalization. Use of an existing 50 kgauss magnet at a field of 10 kgauss to 20 kgauss will populate the magnetic ground state with 20% to 40% of the reemitted positrons. The magnetic fields are such that the high magnetic state positrons have short transit times in the drift tubes and can be excluded from the data analysis. The positrons are reemitted with a center of energy corresponding to their work function in the crystal (~2 eV), and a spread as described above (~0.5×10^{-3} eV). There will be ~10^5 positrons per pulse in the magnetic ground state emitteed from the rethermalizer. Since the interaction time in the rethermalizer is on the order of 10^{-11} sec, the 10^{-8} sec pulse width is unaffected.

The positrons are magnetically guided to the velocity selector tube (see figure 2.1) where the energy spread is reduced further. This is accomplished by using the transit time of a particle through the velocity selector to determine its energy. Knowing the particle energy, a time-dependent voltage can be applied to the velocity selector to offset the known energy (see figure 2.2). In other words, a retarding voltage can be used to slow down the faster particles, so they all leave the velocity selector region with the same kinetic energy. Physically, a fast particle has high energy, so the velocity selector should be a comparatively deep potential well so the particle has a low kinetic energy in the test region. Conversely, a slow particle already has a low energy, so the velocity selector only needs to be a shallow well. In the process of narrowing the energy spread, the pulse is spread over a longer time interval. The reverse of this procedure has been successfully used to time bunch monoenergetic

positrons.[14]

The operation of the velocity selector has been computer simulated. The procedure used was to wait until the particle pulse was in the velocity selector and then start varying the voltage of the velocity selector. Nominally, the energy is given by

(4) $E = 1/2\ mL^2t^{-2}$,

where L is the length of the velocity selector, and t is the transit time. The form chosen for the applied potential was

$$(5)\quad V(t) = \begin{cases} \alpha & t < t_0 \\ \alpha \left(\frac{t}{t_0}\right)^{-2} & t \geq t_0 \end{cases}$$

where t_0 is chosen to be a time after the pulse has entered the velocity selector, and before the first particles exit. If equation (4) were exact, the appropriate choice of α in (5) would result in all of the particles exiting with the same energy. In actuality, electric field penetration into the velocity selector alters equation (5). Also, the fringe electric fields at the end of the velocity selector tube will be changing in time, so the total energy of the particles will change in time also. Both of these effects are included in the simulation, so the t^{-2} trial function used will result in some energy spread in the final distribution. Figure 2.3a shows the energy distribution incident on the velocity selector. It is a gaussian with a width of 0.5 meV and is centered at 1.0 meV. Figure 2.3b shows the resulting energy distribution when α was chosen ignoring the corrections to (4). The width is approximately 35 μeV . Figure 2.3c shows the result of raising the incident center of energy to 2.5 meV and chosing α to minimize the energy spread. Now the width is only a few μeV. A more complicated trial function in equation (5) would result in a more symmetric, narrower energy distribution. In both cases $t_0 = 20\ \mu s$ and the pulse is spread to ~10 μs wide.

There are several factors which tend to increase the spread in the output energy distribution. One is Johnson (thermal) noise on the electrodes. The Johnson noise in the present system is below 10^{-11} μV. The noise on the velocity selector will be higher due to the time varying voltages, but can still be kept below 10^{-7} V through the use of superconducting electronics and appropriate circuit design. This will not limit the velocty selector effectiveness.

This method of reducing the energy spread requires synchronization between the application of the time-varying voltage and the entrance of the pulse into the velocity selector. The timing errors in the electronics should be less than 10 nanosecond, and there will be a 10 nanosecond uncertainty due to the pulse width. For a 0.5 meV wide distribution centered at 1.0 meV, these timing errors will spread the final distribution by 0.3 μeV and should not be a limitation on the technique.

If there are patch effect fields in the velocity selector, the transit time will be changed. If t is the transit time without patches, then the modified transit time, t', is[11]

$$(6) \qquad t' \approx t\left[1 + \frac{3\langle\Phi^2\rangle}{8E^2}\right] \qquad E >> \langle\Phi^2\rangle$$

where E is the particle's energy. For $\langle\Phi^2\rangle \approx 10^{-6}$ V determined earlier, and $E = 10^{-3}$ eV used here, $(t' - t) = 2\times10^{-11}$ sec. This is much less than the 10^{-8} sec timing uncertainties, hence negligible.

Overall, the velocity selector should be able to narrow the energy spread of the exiting particles to ~10^{-6} eV. When used with the LLNL linac positron source, this will result in 10^5 usable positrons per pulse. The calculations in the next sections assume only a one meV wide distribution (typical of the rethermalizer), so use of the velocity selector will allow us to obtain more accurate results in a shorter time than is calculated there.

The modifications we propose include installing the velocity selector and modifying the magnet system and detector location to use an external source of particles. These changes will be tested by using an electron cathode in place of the positron rethermalizer. The current electron

cathode has an energy spread of ~0.5 eV, and produces ~10^9 electrons per pulse, so the number of low energy electrons would be essentially the same as for the positron source. This will allow us to verify the original measurement of g for the electron (by the movable drift tube technique), and to obtain the electron measurement needed to calibrate the TOF technique. The following sections discuss these two techniques in detail.

SECTION 3 - THE TIME OF FLIGHT MEASUREMENT

In its simplest form, the measurement of the gravitational acceleration of the electron (positron) requires only a knowledge of the time in which the particle falls (or rises, because of some initial velocity) in a gravitational field. But because of the weakness of the gravitational interaction (a change in energy of 5.5×10^{-11} eV over one meter), there are practical difficulties. The large ratio of the electromagnetic interaction to the gravitational interaction at laboratory scales requires that the charged particle traverse a test region that is field-free to a high degree of accuracy. This is the purpose of the drift tubes.

We have manufactured very regular cylindrical coppper tubes to shield particles on the axis from stray electric fields. Yet this device itself creates stray fields because its surface is *not* at an equal electrostatic potential. Due to a polycrystalline surface, rms fluctuations on the order of 10^{-6} volts will be found on the axis of a five centimeter diameter metal tube[11]. These are much larger than the gravitational energy scale mentioned above and tend to mask the gravitationally induced change in time of flight. However, a low temperature shielding that reduce these fluctuations to a negligible level has been reported by Witteborn and Fairbank[1,3,6] and Lockhart, Witteborn, and Fairbank[4]. (See also section 1 of this proposal). We complete the analysis of this section assuming that stray fields are completely shielded. (Although see section 4 for a measurement technique that is independent of the patch effect fields).

Since the incident beam cannot be strictly monoenergetic, electrons do not arrive at the detector simultaneously, but with a particular time dependence. For sufficiently low energy electrons (those with energies much less than the energy spread of the incoming beam) we will see that the number versus time curve measured at the detector is very insensitive to the exact energy distribution of the incident pulse. The gravitational force on the particle, however, enters in a way large enough to let us measure the force of gravity on an electron or positron to an accuracy of 1% after approximately three hours of data taking. The rest of this section describes the measurement process in detail, and makes the above estimate of its accuracy.

We can write the position dependent electron (positron) kinetic energy as

$$\frac{1}{2}m\left(\frac{dz}{dt}\right)^2 = \frac{1}{2}mv_0^2 + mgz$$

where v_0 is the initial velocity of the particle. (The particle is directed downward here, as is the z axis). This equation can be integrated to give the time of flight as a function of initial energy, and then inverted to give initial velocity as a function of time:

$$t = \frac{v_0}{g}\left[\left(1 + \frac{2gl}{v_0^2}\right)^{\frac{1}{2}} - 1\right] \quad ; \quad v_0 = \frac{l}{t} - \frac{gt}{2}$$

We therefore see that there is a maximum time of flight t_{max} given by

$$t_{max} = \left(\frac{2l}{g}\right)^{\frac{1}{2}}$$

which corresponds to the time of flight of a particle with zero initial velocity as it is accelerated down the gravitational well. For g of 9.8 m/s^2 and a length l of one meter, t_{max} is 0.45 seconds.

The particles leaving the thermalizer (see section 2) have a Maxwell distribution of velocities[14]

$$P(v_z) = \frac{1}{\sigma\sqrt{2\pi}}\, e^{-\frac{v_z^2}{2\sigma^2}}$$

where σ is the thermal velocity spread, which for electrons at 4.2 K is 7.8 x 10^3 m/s. From the relation

$$P(t < t_0) = P\left(v_0 > \frac{l}{t_0} - \frac{gt_0}{2}\right)$$

we find the probability density for the time of flight by taking a derivative with respect to t_0:

$$P(t) = \begin{cases} \frac{1}{\sigma\sqrt{2\pi}} \left(\frac{l}{t^2} + \frac{g}{2} \right) \exp - \left(\frac{l}{t} - \frac{gt^2}{2} \right)^2 / 2\sigma^2 & t < \left(\frac{2l}{g} \right)^{\frac{1}{2}} \\ 0 & \text{otherwise} \end{cases}$$

Therefore the mean number of particles detected in the time interval δt around t is

$$\langle N(t) \rangle = N_{tot} P(t) \delta t$$

where N_{tot} is the total number of particles.

The above expression for P(t) is relatively complicated, but it simplifies when we consider only those particles with time of flights near the cutoff time. Since the velocities corresponding to these long time of flights are small compared with the distribution width σ, the argument of the exponential in P(t) is small. Thus to a very good approximation

$$\langle N(t) \rangle = \frac{N_{tot}}{\sigma\sqrt{2\pi}} \delta t \left(\frac{l}{t^2} + \frac{g}{2} \right)$$

We find the gravitational force on the electron (positron) by fitting this form to the data and extracting g from the coefficients. This is a simple linear regression problem in t^{-2}, but because N_{tot} and σ are not known to a high degree of accuracy we fit both the intercept and the slope, then divide to find g :

$$\langle N(t) \rangle = \frac{b_1}{t^2} + b_0 \qquad ; \qquad g = -2l \frac{b_0}{b_1}$$

In order to find the expected error in measuring g with this method, we need to know the width of the distribution N(t) for particular times t_0. If the time axis is divided into bins of width δt (with a multichannel analyzer), a particle will be found in bin t with probability $P(t)\delta t$ and in any of the remaining bins with probability $1 - P(t)\delta t$. Thus the probability that N(t) particles arrive in bin t out of a total number of particles N_{tot} is binomially distributed with mean $\langle N(t) \rangle = N_{tot} P(t) \delta t$ and variance $\langle N^2(t) \rangle = \langle N(t) \rangle (1 - \langle N(t) \rangle / N_{tot})$. For $N(t) \ll N_{tot}$ (small bin size) this becomes a Poisson distribution, which approaches a gaussian as N_{tot} gets large. This gaussian has

variance $\sigma^2(t) = \langle N(t) \rangle$. We solve for the coefficients b_0 and b_1 using the method of weighted least squares[15], finding the variance matrix of the coefficient vector to be

$$\frac{1}{\Delta}\begin{bmatrix} \Sigma(t_i^2\sigma_i)^{-2} & -\Sigma(t_i^2\sigma_i)^{-2} \\ -\Sigma(t_i^2\sigma_i)^{-2} & \Sigma\sigma_i^{-2} \end{bmatrix} = \begin{bmatrix} \sigma_{b_1}^2 & \sigma_{b_1 b_0} \\ \sigma_{b_0 b_1} & \sigma_{b_0}^2 \end{bmatrix}$$

where

$$\Delta = \Sigma\sigma_i^{-2}\Sigma(t_i^2\sigma_i)^{-2} - (\Sigma(t_i\sigma_i)^{-2})^2$$

With these variances and covariances (b_0 and b_1 are correleated) we find the uncertainty in g (calculated from $g = -2l/b_0/b_1$) using the method of propagation of errors. If we divide the time axis into 100 bins between 0.2 and 0.4 seconds, one calculates in this way that a 1% error in the value of g can be obtained with 10^9 particles falling a distance of one meter. This assumes an initial energy width thermalized to 4.2 K as discussed in section 2. With 10^5 particles per pulse (section 2) and a repetition rate of one second to allow the long time of flight electrons to arrive at the detector, this 1% accurracy level requires 2.8 hours of running time.

We have ignored certain complicating features in the actual experiment because, as we now argue, they do not substantially affect the conclusions. Because the incoming electron (positron) pulse is centered around a nonzero energy (see section 2), we must bias the drift tube in order to operate at the center of the energy distribution, maximising the number of slow electrons. Thus the potential near the entrance of the tube is modified slightly from the form assumed in the kinetic energy equation at the beginning of this section (gravity only), and will affect the time of flight. A further end effect is the image force experienced by the charge as it enters the drift tube[16]. These effects can be calculated to determine what functional form to numerically fit to the the data. Because an analytic fitting function is not available, the error cannot be caluculated using the linear regression formalism developed here, although the accurracy to which we can extract g will remain substantially the same.

SECTION 4 - THE MOVABLE DRIFT TUBE MEASUREMENT

The method to measure the electron (positron) gravitational acceleration that we have just described uses the time of flight chartacteristics of slow electrons, and hence relies on the low temperature shielding effect to screen patch effect fields as observed in the original low temperature experiments[3,6]. However, an alternative method using a second, movable drift tube has been demonstrated to measure the gravitational acceleration of the electron even with an unshielded patch effect[1,4] (see section 1). This section of the proposal describes the measurement in detail, showing that a 1% measurement of the gravitational acceleration of the positron can be obtained in three hours using the positron linac at LLNL. (Similar results can be obtained with electrons at Stanford).

The measurement involves finding the potential difference between the movable and fixed tubes that maximises the number of slow particles seen at the detector for a given tube separation. This method uses the fact that both both the upper (fixed) and lower (movable) drift tubes have a region along the axis of maximum potential (due to the patch effect) that acts as a barrier to the electron pulse and moves with the tubes. Now, the number of particles arriving after some time t_0 is equal to the number in the pulse with initial velocity less than $v(t_0)$, the velocity needed to traverse the two tubes in time t_0. Suppose that the two tubes are biased so that their potential maxima are of equal height. When the barrier height of the movable tube is lowered, the initial velocity required to traverse this new potential in time t_0 becomes smaller. Hence the number of particles arriving after this time has decreased. The number also decreases as the movable tube is raised in potential, as can be seen from considering the two tubes in opposite order. Thus the number of particles arriving at the detector after some time t_0 is a maximum when the barrier heights of the tubes are equal.

Suppose now that the separation of the tubes is changed from a configuration where the applied potential difference is such that the barrier heights are equal. The particle will gain kinetic energy from gravitational acceleration through the additional distance between the barriers. Then

the energy of the particle relative to the first barrier is no longer equal to its energy relative to the second, decreasing the number of slow particles. The applied potential necessary to again maximise the number of slow particles is equal to $mg\Delta h$, where Δh is the change in tube separation. Since we are sensitive only to changes induced by changing the tube separation, this measurement is independent of the patch field and gravitational sag effects mentioned earlier, since they move along with the tube.

There is, however, another effect when the two tubes are connected with a wire, as they must be to control their relative potentials. Before the drift tubes are connected, they are not in thermodynamic equilibrium because the gravitational potential terms in the free energies are different. When they are connected, charge flows between the tubes, creating an electrostatic potential that exactly cancels the difference in gravitational energies. This can be seen more clearly from Fig. 4.1. Consider a particle moving from the region of highest potential in the upper (fixed) tube (point A) to the region of highest potential in the movable tube (point B) along the path AB. If we take the particle from point B, through the surface of the lower drift tube, through the wire and into the upper tube, then out through the surface to its original position at point A, we can have done no work in the conservative potential. Since no work is done in moving from point C to point D (the metals are in equilibrium under electron exchange), and the work done in moving from D to A and from B to C is independent of tube separation, the work done in moving the electron from point A to point B must be independent of the tube separation. Hence the energy of the electron relative to the movable drift tube's potential maximum is independent of tube position, and no additional potential is required to stop the beam from reaching the detector when the tube separation is increased. But the electrostatic potentials that cancel the force of gravity on an electron add to gravity for the oppositely charged positron, resulting in a net measured acceleration of $2g$ if the gravitational mass of the electron and positron are equal.

We now show that additional complications due to stray electric fields and non-axial particle trajectories can be made small enough to measure the gravitational acceleration of our test particles with this method. Because the two drift tubes are within a third, larger, shielding tube, there are

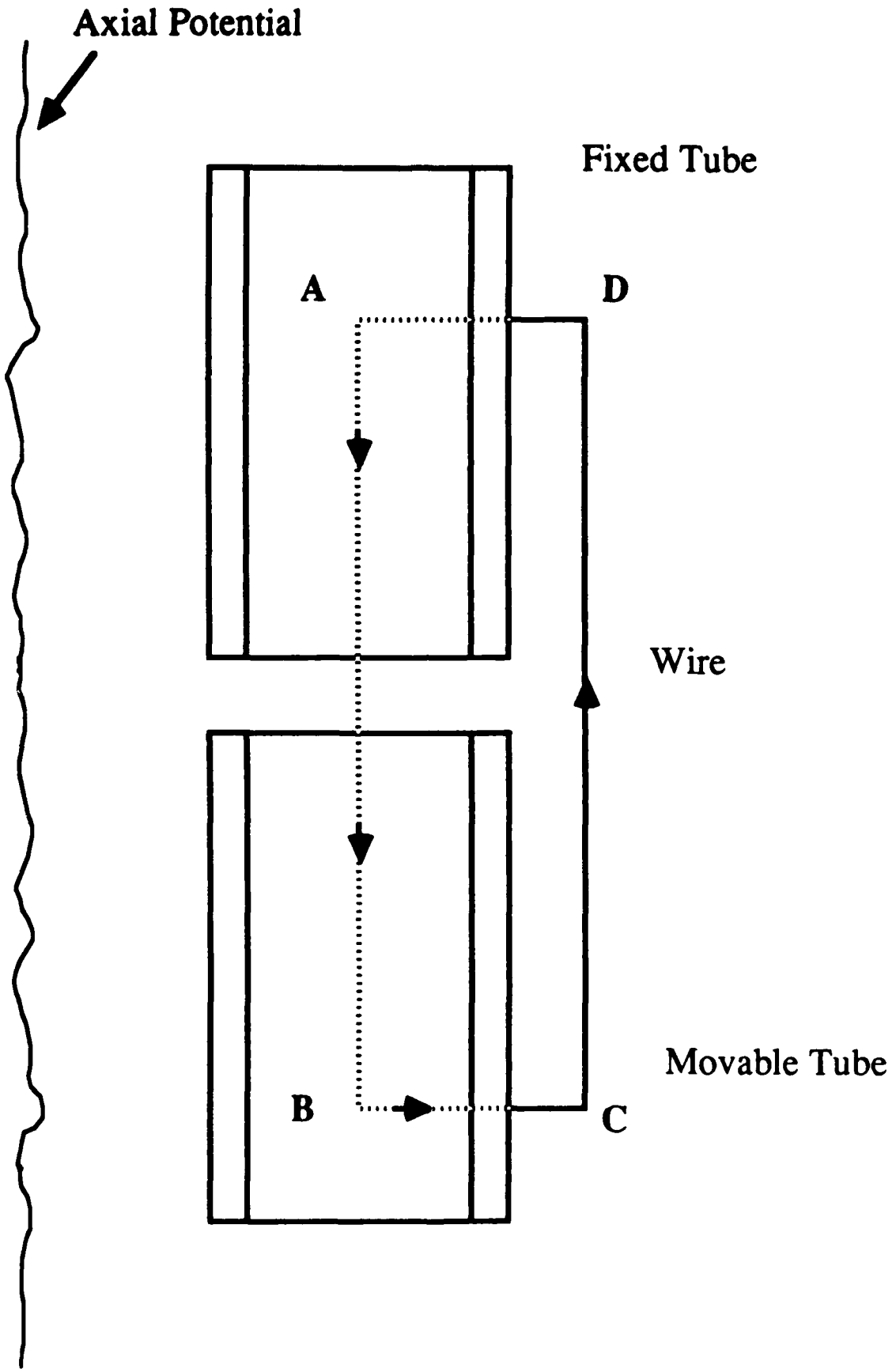

Fig. 4.1 Conservation of energy argument for the movable drift tube experiment (see text).

random electric fields generated by its surface which do not move along with the movable drift tube. These can in principle change the height of the movable potential barrier and introduce a systematic error. But we can now make use of the static shielding properties of a metal cylinder. Far inside a very long cylinder, these stray fields would be attenuated to zero; it is only field penetration at the ends that poses a possible problem. The quantity of interest is the amount that the external fields have been attenuated at the position of the potential maximum of the movable drift tube, which we can easily estimate as follows.

Suppose that both drift tubes are biased at a negative (positive) voltage so that the electrons (positrons) move with relatively high energy through the approximately zero potential region separating them. As the particles enter the movable drift tube (see Fig. 4.2), the potential is rising toward its asymptotic average value deep inside the cylinder. Even in the asymptotic region, however, it fluctuates around the average with an rms deviation σ. One can see from Fig. 4.2 that the particles entering the movable drift tube will not encounter a fluctuation large enough to turn them back until the axial potential has risen to within σ of its asymptotic average. Since this rms deviation σ is on the order of 10^{-6} volts[11], we see that biasing the tube at a potential of ten volts means that the particle will not be turned around until it is in a region where external fields are attenuated by a factor of 10^{-7}. Since we expect ambient potential fluctuations generated by the larger, outside tube to be also on the order of 10^{-6} volts, we see that possible offsets are attenuated to a level of 10^{-13} volts - a small fraction of the 5×10^{-11} volt gravitational potential change of an electron over one meter.

Another possible difficulty is that since the test particles are not confined exactly to the axis of the drift tubes, the maximum potential along different paths can vary slightly. This effect is independent of tube separation and is easily seen to be equivalent to a variation in the initial energy of the particle. Since the patch effect potentials have a correlation length on the order of the tube radius[5], we see that any variation in particle trajectory will most probably be much less than the rms fluctuation level of 10^{-6} volts, and certainly no larger than this. We will find later that an initial energy spread of 10^{-3} volts in the electron pulse is adequate to give accurate measurements of the

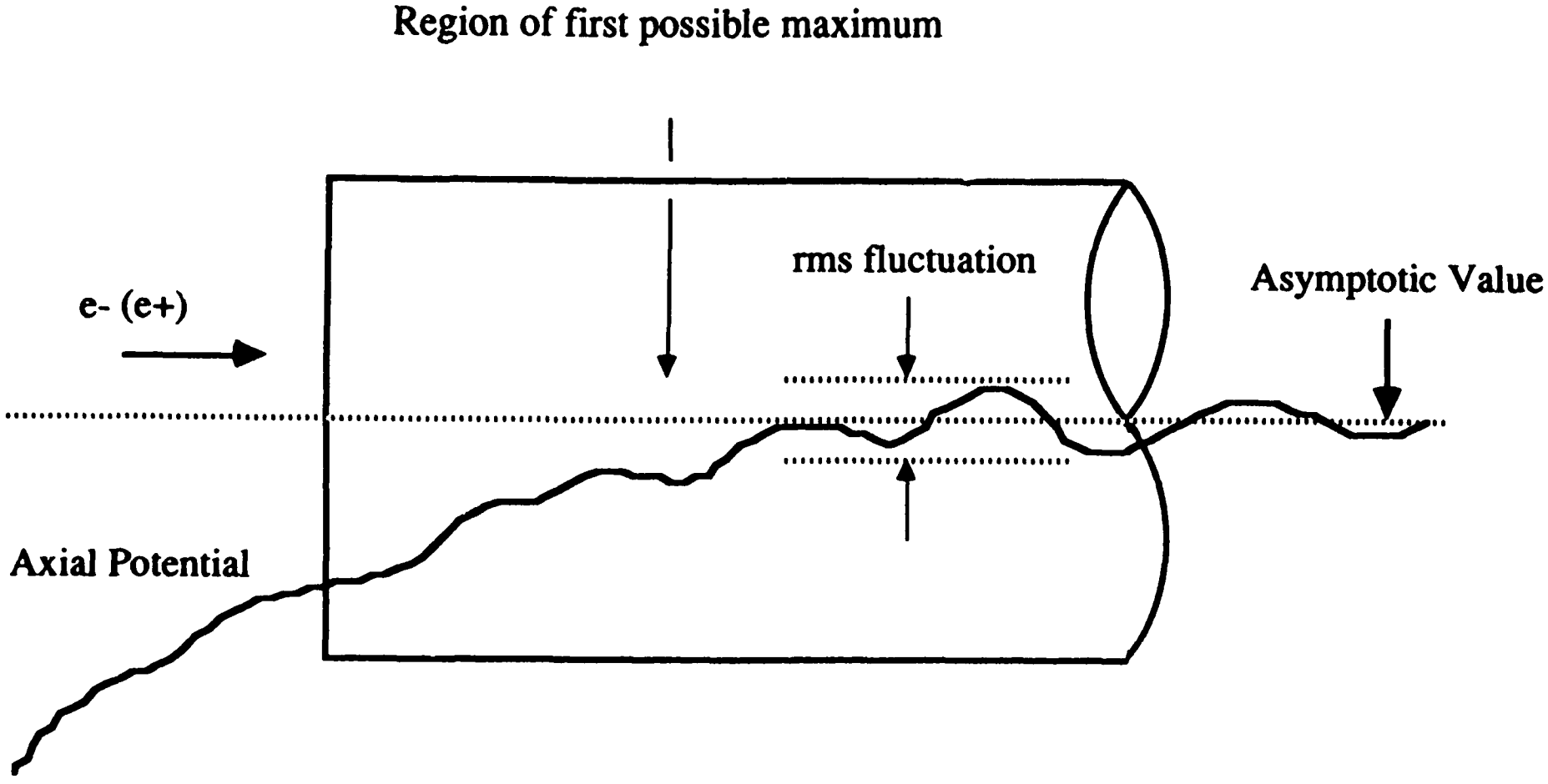

Fig. 4.2 Shielding of stray fields in the movable drift tube experiment (see text).

gravitational mass of electron (positron): therefore the effect due to different particle paths can be absorbed into an initial energy spread with little loss of accuracy.

We have shown that the systematic errors are small, but the problem remains that the number of incoming particles in the velocity range of interest fluctuates because of the energy spread of the incoming beam. We can reduce this error by averaging over many incident pulses. The running time necessary for such an average to yield an accurate measurement of g can be calculated in the following way.

If $v(t_0)$ is the initial velocity required for a particle to traverse the two drift tubes in time t_0, then the probability that a particle reaches the detector after time t_0 can be written

$$P(t > t_0) = P(v < v(t_0)) \approx \frac{v(t_0)}{\sigma\sqrt{2\pi}} \qquad v(t_0) << \sigma$$

where we have used the same Maxwell distribution for the incident velocities as in section 3. The last equality holds because, as in section 3, we consider only particles with velocities much less than the width σ of the velocity distribution. In this region, the distribution is flat to a very good approximation. If the total number of particles is N_{tot}, then the mean number arriving after time t_0 is

$$\langle N(t > t_0) \rangle = \frac{N_{tot}}{\sigma\sqrt{2\pi}} v(t_0)$$

Suppose that a particle moves through the potential of fig. 4.3 . For anlaytic convenience we assume that the particle moves quickly between the regions of drift tube maxima, and that the maxima of the two tubes are of identical shape. (These conditions are not crucial to the experiment, but allow us to present a concise derivation of the expected sensitivity.) The total time of flight is then the sum of the time of flights in regions I and II:

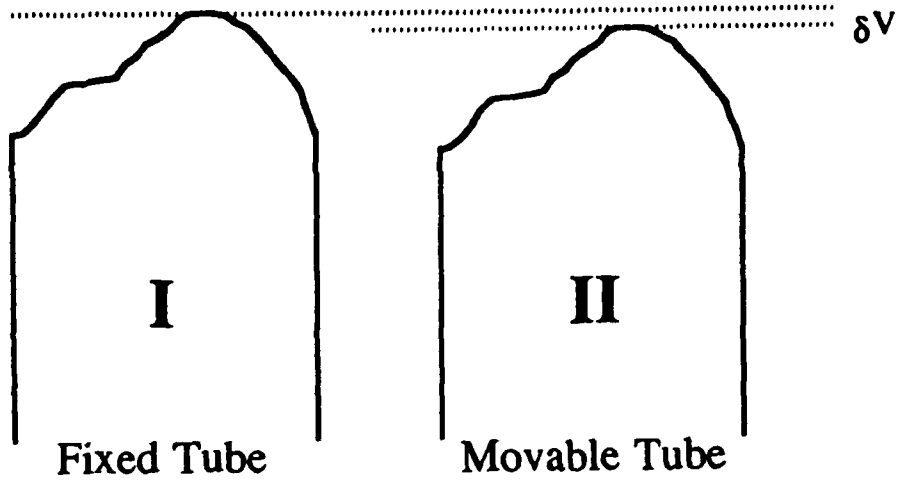

Fig. 4.3 Potentials in the two tube syste, contributing to the measured time of flight (see text). The time of flight is maximized for δV equal to zero.

$$t_0 = \int \frac{dz}{\sqrt{v_0^2 + \frac{2}{m}V(z)}} + \int \frac{dz}{\sqrt{v_0^2 + \frac{2}{m}V(z) + \alpha}}$$

$$\equiv f(v_0^2) + f(v_0^2 + \alpha)$$

Here V(z) is the shape of the potential maxima and α is equal to $2/m\delta V$, where δV is as in fig.4.3. If we could invert this relation, we would write

$$< N(t > t_0) > = \frac{N_{tot}}{\sigma\sqrt{2\pi}} v(t_0, \alpha)$$

As discussed at the beginning of this section, $< N(t > t_0) >$ is a decreasing function of $|\alpha|$ with a maximum at $\alpha = 0$. To know how accurately we can determine this maximum, we must calculate the sensitivity of $< N(t > t_0) >$ to a change in α. Using the chain rule,

$$\frac{d}{d\alpha} < N(t > t_0) > \Big|_{\alpha=0} \delta\alpha = \frac{N_{tot}}{\sigma\sqrt{2\pi}} \left(\frac{dt}{dv}\right)^{-1} \left(\frac{dt}{d\alpha}\right)\Big|_{\alpha=0} \delta\alpha$$

The assumption of identical potential maxima, leading to the expression for *t* in eqn. ( ), gives a very simple form for this result, letting us write

$$\Delta < N(t > t_0) > = -\frac{N_{tot}}{\sigma\sqrt{2\pi}} \frac{1}{4\, v(t_0, \alpha=0)} \delta\alpha$$

The limit of detectability is determined by setting this change equal to the standard deviation of the total number of particles detected after time t_0. Since $N(t > t_0)$ has a standard deviation propotional to the square root of the mean,

$$\frac{\Delta < N_{tot}(t > t_0)}{s.d} = \delta\alpha \left(\frac{N_{tot}}{\sigma}\right)^{\frac{1}{2}} \frac{(2\pi)^{\frac{1}{4}}}{4} v^{-\frac{3}{2}}(t_0) = 1$$

The unknown quantity is still $v(t_0)$, since this depends on the exact potential that the particle traverses. However, we can make an estimate of the running time needed to make a 1% measurement of *g* at the 1 σ level by considering a t_0 such that $1/2mv^2(t_0) = 10^{-10}$ eV. For a σ of

7.8×10^3 m/s (corresponding to a distribution thermalized to 4.2 K), this requires 10^9 particles to resolve a δV of 10^{-13} eV. This is 1% of g for a tube displacement of 20 cm. This is the same number of particles as we required in section 3, where we saw it to correspond to three hours of running time.

SECTION 5 - INVE :IGATIONS OF THE LOW TEMPERATUE SHIELDING EFFECT

In section 3 we described a time of flight measurement of the electron and positron gravitational acceleration. This method requires that the stray electric fields on the axis of the cylindrical drift tube be quite small, much smaller, in fact, that one might reasonably expect. The observations of Witteborn and Fairbank[3,6] and of Lockhart, Witteborn and Fairbank[4] suggest that the ambient electric field inside the metal drift tube is unusually small at 4.2 K. Theoretical models have been suggested by Bardeen[17] and Hanni and Madey[18] to account for this. The models propose that a layer of electrons bound to the oxide layer on the metal surface become conducting at low temperature, so that the mobility is high enough to screen variations in the surface potential. Calculations show[18] that electron densities on the order of 10^{12} electrons / cm^2 will substantially screen potential variations on the metal surface.

Because of the importance of such an effect to the time-of-flight measurements, and because of its intrinsic interest as a new solid state phenomenon, we have built two experiments to investigate it more directly. The first of these is a system for high precision measurements of the microwave surface impedance of metals at low temperatures. With this apparatus we have found sharp, anomalous increases in the surface conductivity of copper and aluminum surfaces as the temperature is decreased. Such and anomaly could be generated by an increase in the number of conducting surface electrons. The second experiment is a surface potential probe which can measure directly the local electric fields above a metal surface as a function of position. We propose to modify the first apparatus so that the same samples may be measured in both systems. In this way we may verify, or rule out, whether the phenomenon which causes the anomalies in the surface conductivity reduces the variation in surface potential. We note that recent, independent measurements of the surface potential in an apparatus similiar to ours indicate a dramatic change in the magnitude of the patch effect field at low temperatures[19]; these preliminary measurements have not yet been verified, however.

The microwave cavity system can measure the resonant frequency of a cavity as a function of temperature to better than 1 part in 10^{10} at 9 GHz over the temperature range 2-20 K. The shift in resonant frequency due to a surface conducting layer can easily be computed. For cavities made of pure metals at low temperatures (i.e., in the "extreme anomalous limit" of the surface impedance) one finds that the shift depends only upon the surface carrier density n, the effective mass m, and the scattering time τ

$$\Delta f\,(\mathrm{Hz}) \sim 10^{-12}\left(\frac{m_e}{m}\right) n\ (\mathrm{cm}^{-2}) \times \begin{cases} \omega\tau & \omega\tau \ll 1 \\ 1 & \omega\tau \gg 1 \end{cases}$$

The behavior in other regimes is more complicated, but, in general, changes in the conductivity of a surface layer of 10^{12} - 10^{14} electrons cm^{-2} can be detected. This is a small number compared with the number of surface atoms ($\sim 10^{15}$ cm^{-2}) and a very small number of electrons within the electromagnetic field penetration depth of the surface (10^{18} cm^{-2}).

We have observed sharp changes in the resonant frequency as a fucntion of temperature in cavities made of copper and of aluminum. Of the four copper samples tested (high purity, oxygen-free copper), three showed measurable anomalies. Two of four aluminum samples (6061 aluminum alloy) showed anomalies. All samples had natural oxide layers. Figs. 5.1 and 5.2 show the resonant frequency shift as a function of temperature from two runs, with a background shift due to thermal expansion subtracted. The temperature at which the anomaly appears is sample-dependent, ranging from 3.40 K to 3.85 K. One copper sample showed a second anomaly at a higher temperature, 7.15 K. In all cases the effective surface conductivity increases as the temperature is lowered. The anomalies were stable and reproducible from run to run; the effect on one sample was unchanged after an interval of over a year.

The lower-temperature anomalies are eliminated, and the upper anomaly reduced, by relatively small, static magnetic fields (200 G; see Figs. 5.1 and 5.2). We have also demonstrated

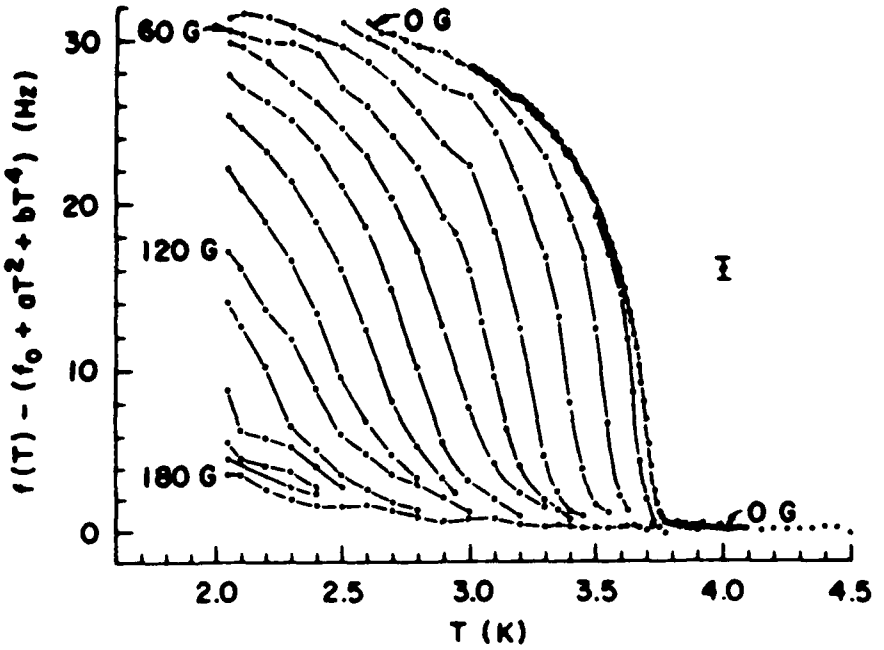

Fig. 5.1 The anomalous frequency shift as a function of temperature for one aluminum sample, with and without a static magnetic field. Thermal expansion has been subtracted by fitting the data above 3.8 K. The magnetic field increases in equal increments of 13.3 G from 0 G (top curve) to about 200 G (bottom curve). Note that the curve in 200 G lies very nearly along the extrapolation of the thermal expansion fit.

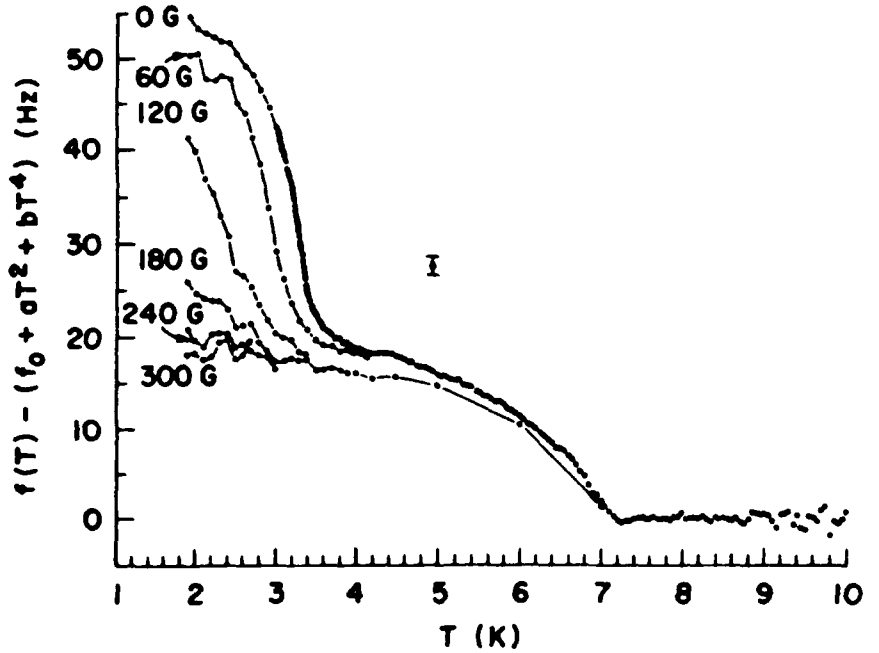

Fig. 5.2 The anomalous frequency shift as a function of temperature for one copper sample with and without a static magnetic. This sample showed two anomalies, one at about 3.6 K and one at 7.2 K.

that the anomalies can be perturbed by deliberate contamination of the surface; Fig. 5.3 shows the effect of helium, Fig. 5.4 oxygen, and Fig. 5.5 a hydrocarbon grease. We believe we have ruled out the possibility of any superconducting contamination.

The second apparatus is an instrument to measure the local surface potential on metal surfaces at low temperature and ultrahigh vacuum as a function of temperature. This apparatus is shown in fig. 5.6. A rotating electrode forms a capacitor with the sample, which is mounted below it on an adjustable stage. The changing voltage across this capacitor as the electrode moves to a region of different sample surface potential causes charge flow to and from the sample. This signal is converted to a voltage by the low temperature amplifier and averaged over 1000 rotations. The result is a measurement of the surface potential along an annulus (see fig. 5.7). Since we are trying to detect an effect that would manifest itself by shielding spatial variations in the surface potential, the sensing area must be kept small. But the voltage sensitivity varies inversely as this sensing area because of the capacitive coupling to the signal. We presently operate with a spatial sensitivity of one millimeter and a voltage sensitivity of one millivolt. Two polycrystalline copper samples, one annealed to grow crystallites large enough to generate resolvable potential changes above the surface, have been measured at temperatures down to 2.9 K. Neither showed evidence of a shielding effect at the present limit of sensitivity. In the microwave cavity experiment, however, we know that the low temperature anomaly did not appear on all samples at the original level of sensitivity, or at all on some. It would therefore be extremely desirable to measure in this apparatus a sample that was known to have an anomaly in its microwave conductivity.

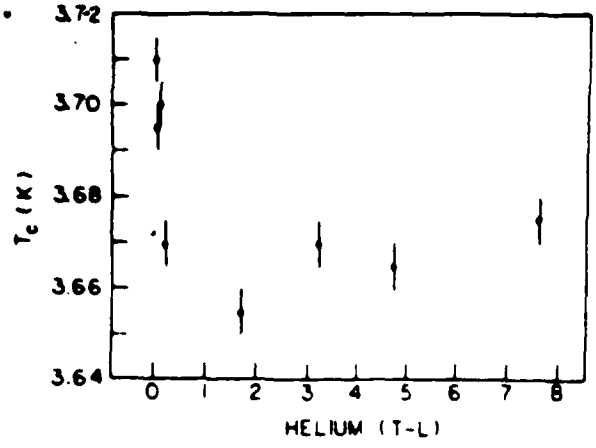

Fig. 5.3 The decrease in the anomaly temperature as helium gas is added to the system. The points shown correspond roughly to 0, 1, 2, 4, 28, 54, 79, and 127 monolayers of helium over the entire vacuum system surface.

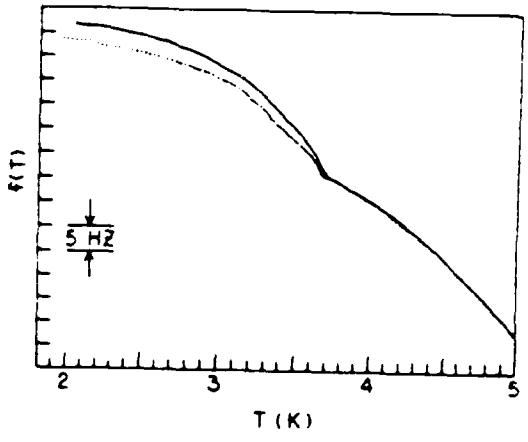

Fig. 5.4 The effect of a film of solid oxygen on the anomaly. Solid line, the frequency shift for a clean coper cavity. Dotted line, the same cavity with about 25,000 monolayers of oxygen on its interior surfaces.

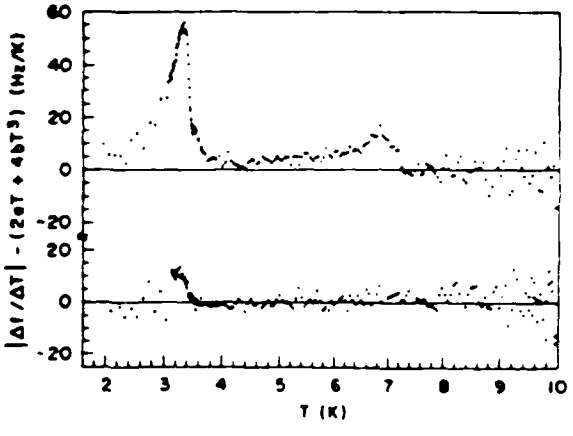

Fig. 5.5 The derivative of the frequency shift for the copper cavity of fig (5.2) with thermal expansion subtracted. Top curve, cavity clean. Bottom curve, the same cavity with vacuum grease on its interior surfaces. The same thermal expansion fit has been subtracted in both cases.

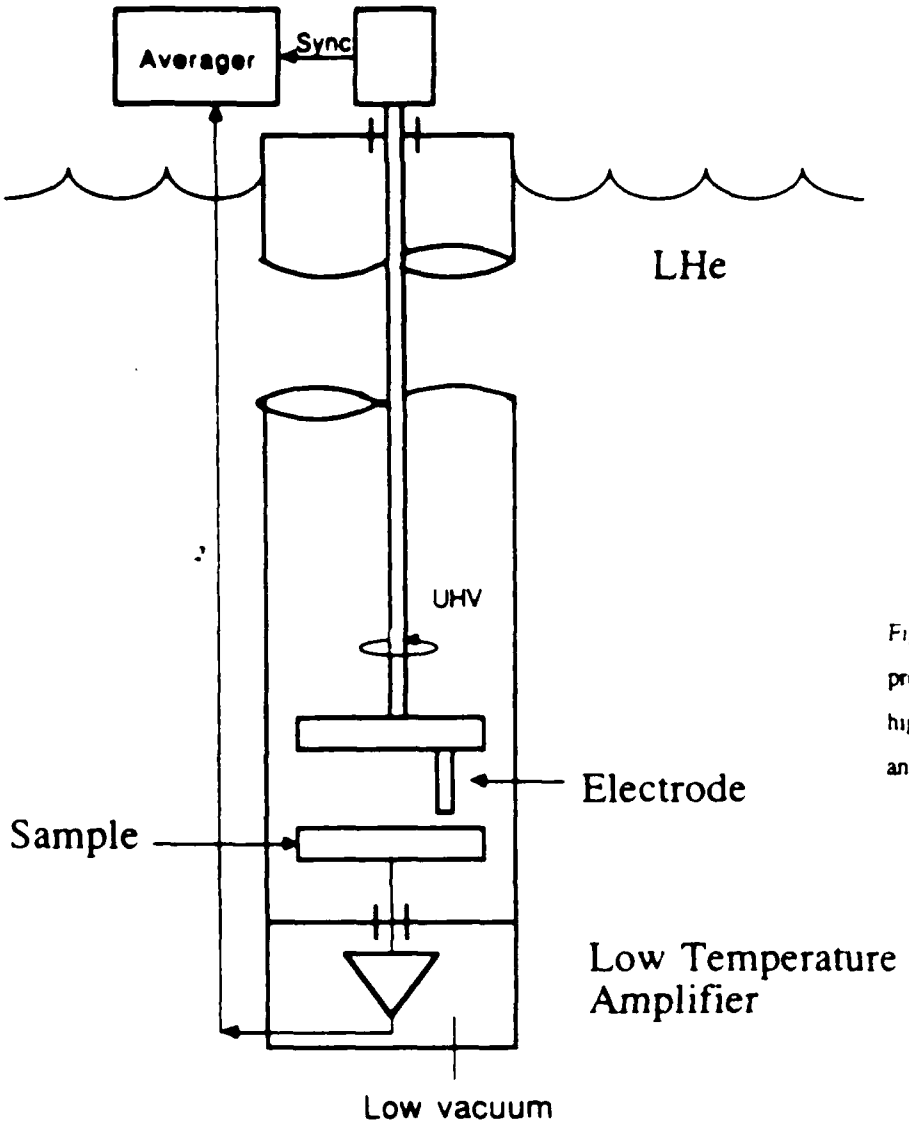

Fig. 5.6 Schematic diagram of the surface potential probe. The electrode rotates above the sample in ultra high vacuum, measuring the surface potential along an annulus. The sample reaches temperatures of 2.9 K.

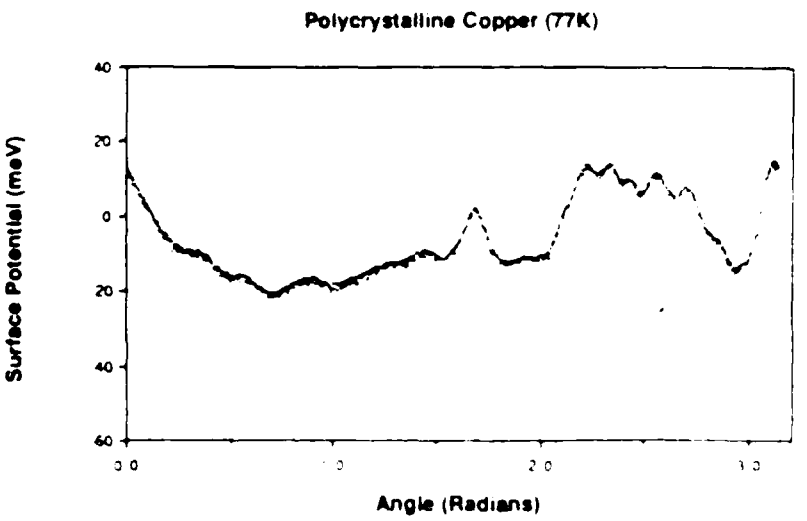

Fig. 5.7 Recent data taken at 77 K. The structure shows large crystallites in the sample (annealed at 1000 C for six hours). The voltage resolution is one meV with a one millimeter spatial resolution.

REFERENCES

1. F. C. Witteborn and W. M. Fairbank, Rev. Sci. Instrum. 48, 1 (1977).

2. T. Goldman and M. M. Nieto, Phys. Lett. 112B, 437 (1982),
   J. Scherk, La Recherche 8, 878 (1977); Phys. Lett. 88B, 265 (1979),
   J. Scherk in Unification of the Fundamental Particle Interactions, eds. S. Ferrara, J. Ellis, and P. van Nieuwenhuizen, Plenum, New York (1981)

3. F. C. Witteborn and W. M. Fairbank, Nature 220, 436 (1968).

4. J. M. Lockhart, F. C. Witteborn and W. M. Fairbank, Phys. Rev. Lett. 38, 1220 (1977)

5. R. H. Howell, R. A. Alvarez, and M. Stanek, Appl. Phys. Lett. 40, 751 (1982).

6. F. C. Witteborn and W. M. Fairbank, Phys. Rev. Lett. 19, 1049 (1967).

7. H. J. Maris, Phys. Rev. Lett. 33, 1177 (1974).
   H. J. Maris, Phys. Rev. Lett. 33, 1594 (1974).

8. L. I. Schiff and M. V. Barnhill, Phys. Rev. 151, 1067 (1966).

9. A. J. Dessler, F. C. Michel, H. E. Rorschach, and G. T. Trammel, Phys. Rev. 168 , 1361 (1968).

10. C. Herring, Phys. Rev. 171, 1361 (1968).

11. M. S. Rzchowski and J. R. Henderson, *The effect of spatially random fields on time-of-flight spectroscopy*, in preparation.

12. R. H. Howell, M. J. Fluss, I. J. Rosenberg, and P. Meyer, Nucl. Instr. and Methods, B10/11, 373 (1985).

13. B. L. Brown, W. S. Crane, and A. P. Mills, Jr., Appl. Phys. Lett. 48, 739 (1986).

14. A. P. Mills, Jr., Appl. Phys. 22, 273 (1980).

15. B.R. Martin, Statistics for Physicists, Academic Press, London (1971).

16. F.C. Witteborn, Ph.D. Thesis, Stanford University (1965), unpublished.

17. J. Bardeen, "Comments on Shielding by Surface States," to be published in Near Zero: New Frontiers in Physics, C.W.F. Everittt, ed. (Freeman, 1986).

18. R.S. Hanni and J.M.J. Madey, Phys. Rev. B 17, 1976 (1978).

19. G.I. Opat, University of Melbourne, private communication.

APPENDIX D

Submitted to LT-13 - to be published in the Japanese Journal of Applied Physics.

Indications of a High Mobility Surface Layer on Oxidised Copper and Aluminum Surfaces at Low Temperatures

M.S. RZCHOWSKI, R.W. RIGBY, and W.M. FAIRBANK

Physics Department, Stanford University, Stanford, CA 94305, USA

We discuss progress in the comparison of the temperature dependence of the microwave surface impedance and of the spatial variations in the surface potential on oxidized copper and aluminum. These measurements test the hypothesis that sharp increases in the microwave surface conductivity of copper and aluminum are caused by the appearance of a high mobility surface layer at low temperatures. An *in-situ* evaporator in our UHV surface potential apparratus will allow work function measurements of well-characterized surfaces, but the samples must be transferred in air to the surface impedance experiment.

1. INTRODUCTION

In the models suggested by Bardeen[1] and Manni and Madey[2] to explain the absence of large electric "patch effect" fields[3,4,5] above a polycystalline metal surface, a layer of electrons bound to the surface oxide layer of a metal becomes conducting at low temperatures. Calculations show[2] that electron densities on the order of 10^{12} electrons / cm^2 will substantially screen potential variations on the metal surface.

We have constructed two experiments to investigate this effect more directly. The first of these is a system for high precision measurements of the microwave surface impedance of metals at low temperatures. With this apparatus we have found sharp, anomalous increases in the surface conductivity of copper and aluminum surfaces as the temperature is decreased. Such anomalies would be generated by an increase in the number of conducting surface electrons. The second experiment is a surface potential probe which can measure directly the local electric fields above a metal surface as a function of position. We report here on modifications of the microwave cavity apparatus to accept samples compatible with the surface potential apparatus.

Examining the same samples in both experiments indicates whether the surface impedance anomalies are in fact caused by an additional surface conducting layer capable of screening surface potential variations.

2. EXPERIMENTAL DETAILS

The microwave cavity system can measure the resonant frequency of a cavity as a function of temperature to better than 1 part in 10^{10} at its resonant frequency of 9 GHz over the temperature range ?-20 K. For cavities made of pure metals at low temperatures (i.e., in the "extreme anomalous limit" of the surface impedance) one finds that the shift depends only upon the surface carrier density n, the effective mass m, and the scattering time τ

$$\Delta f(\mathrm{Hz}) \sim 10^{12}\left(\frac{n_s}{m}\right) s\,(\mathrm{cm}^2)\,\Omega \begin{cases} \omega\tau & \omega\tau \ll 1 \\ 1 & \omega\tau \gg 1 \end{cases}$$

In general, changes in the conductivity of a surface layer of 10^{12} - 10^{14} electrons / cm^2 can be detected.

We have observed sharp changes in the resonant frequency as a function of temperature in cylindrical cavities made of copper and aluminum. The effective surface conductivity increases as the temperature is lowered. The anomalies were stable and reproducible from run to run; the effect on one sample was unchanged after an interval of over a year.

Figure 1 shows the frequency shift as a function of temperature for several magnetic fields applied along the axis of the cavity. The effect of the field is strongly temperature dependent, with the suppression largest at higher temperatures. A field of 200 gauss suppresses the anomaly almost entirely, bringing the f(T) curve very near to the extrapolation of the fit to the thermal expansion form above the anomaly.

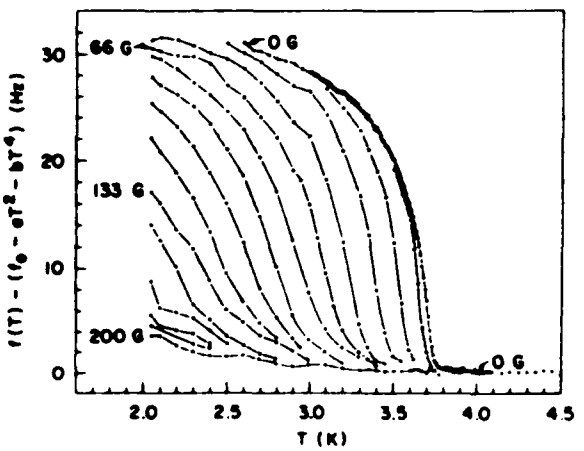

Fig. 1. Resonant frequency of the microwave cavity as a function of temperature in different axial magnetic fields. The thermal expansion background has been fit and subtracted.

Since the appearance of a surface conducting layer would reduce the spatial variation of the surface potential as discussed earlier, we have developed a work function apparatus operating in UHV and at cryogenic temperatures. A rotating electrode forms a capacitor with the sample, which

is mounted below it on an adjustable stage. The changing voltage across this capacitor as the electrode moves to a region of different sample surface potential causes charge flow to and from the sample. This signal is converted to a voltage by the low temperature amplifier and signal averaged. The result is a measurement of the surface potential along an annulus (see fig. 2). Cryogenic temperatures are obtained by immersing the probe in liquid helium.

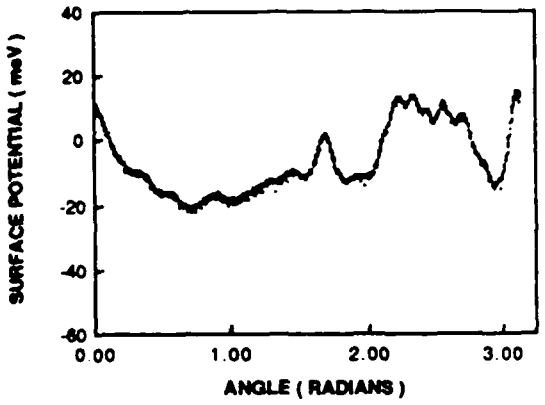

Fig. 2. The 77 K surface potential along an annulus of polycrystalline copper annealed at 1000 C for six hours, resulting in macroscopic crystallites. Sample temperatures of 2.9 K are attained in the surface potential apparatus.

We presently operate with a spatial sensitivity of one millimeter and a voltage sensitivity of one millivolt. Two polycrystalline copper samples, one annealed to grow crystallites large enough to generate resolvable potential changes above the surface, have been measured at temperatures down to 2.9 K. Neither showed evidence of a shielding effect at the present limit of sensitivity. In the microwave cavity experiment, however, we know that the low temperature anomaly did not appear on all samples at the original level of sensitivity, or at all on some.

3. DISCUSSION

We have ruled out a number of explanations for the anomalies. However, the possibility of a superconducting contaminant cannot be completely eliminated at this time. We have deliberately introduced a superconducting contaminant, and observed frequency shifts and magnetic effects similar to those described above. But the amount of contaminant must be quite large - about 10^{-2} cm^2 for a 50 Hz. shift. Furthermore, we observe a small but clear perturbation to the anomaly with deliberate surface contamination (helium, oxygen, hydrocarbons), which suggest a surface phenomenon. With the modified experiment described below, we can control and analyze the sample purity sufficiently to determine whether a superconducting contaminant is responsible for the conductivity anomalies.

4. FURTHER WORK

We have modified the surface impedance experiment to accept, as a removable insert in the cavity wall, a sample compatible with our surface potential apparatus. The insert and cavity are thermally isolated from one another so that their temperatures can be varied independently. Surface potential measurements of a sample with a surface impedance anomaly would clearly test the existence of a shielding conducting layer of electrons. Preliminary measurements of one insert show no anomalous effect, although the main cavity has a small but clearly recognizable temperature dependent frequency shift (see Fig. 3).

Figure 3 shows the frequency shift on application of a 200 gauss magnetic field. As can be seen in Fig. 1, there is a temperature dependent shift in the resonant frequency with axial magnetic field only below the transition temperature. (In Fig. 3, a shift with magnetic field due to the constant 2.5 K temperature of the main cavity has been subtracted, as well as a temperature independent shift of the insert with magnetic field).The method of Fig. 3 eliminates long term drift, resulting in a more sensitive measurement.

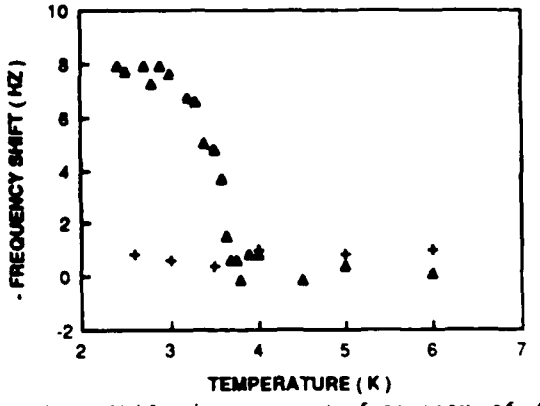

Fig. 3. Shift in resonant frequency of the microwave cavity on application of a 200 gauss magnetic field. The triangles are shifts in the main cavity; the pluses are for the thermally isolated insert (see text).

We are currently installing a resistive evaporator in the surface potential apparatus so that surfaces can be deposited *in-situ* at low temperature. However, samples must be transferred in air to the surface impedance probe.

REFERENCES

1) J. Bardeen, "Comments on Shielding by Surface States," to be published in Near Zero: New Frontiers in Physics, C.W.F. Everitt, ed. (Freeman, 1987).
2) R.S. Hanni and J.M.J. Madey, Phys. Rev. B 17, 1976 (1978).
3) F.C. Witteborn and W.M. Fairbank, Phys. Rev. Lett. 19, 1049 (1967)
4) F.C. Witteborn and W.M. Fairbank, Nature 220, 436 (1968).
5) J.M. Lockhart, F.C. Witteborn, and W.M. Fairbank, Phys. Rev. Lett. 38, 1220 (1977).

END

9-87

DTIC